

A. PAWEŁEK<sup>\*,#</sup>, A. PIĄTKOWSKI<sup>\*</sup>, W. WAJDA<sup>\*</sup>, W. SKUZA<sup>\*</sup>, A. TARASEK<sup>\*</sup>, Z. RANACHOWSKI<sup>\*\*</sup>, P. RANACHOWSKI<sup>\*\*</sup>, W. OZGOWICZ<sup>\*\*\*</sup>, S. KÚDELA JR.<sup>\*\*\*\*</sup>, S. KÚDELA<sup>\*\*\*\*</sup>

## PLASTIC INSTABILITIES INDUCED BY THE PORTEVIN - LE CHÂTELIER EFFECT AND FRACTURE CHARACTER OF DEFORMED Mg-Li ALLOYS INVESTIGATED USING THE ACOUSTIC EMISSION METHOD

The results of the investigation of both mechanical and acoustic emission (AE) behaviors of Mg<sub>4</sub>Li<sub>5</sub>Al and Mg<sub>4</sub>Li<sub>4</sub>Zn alloys subjected to compression and tensile tests at room temperature are compared with the test results obtained using the same alloys and loading scheme but at elevated temperatures. The main aim of the paper is to investigate, to determine and to explain the relation between plastic flow instabilities and the fracture characteristics. There are discussed the possible influence of the factors related with enhanced internal stresses such as: segregation of precipitates along grain boundaries, interaction of solute atoms with mobile dislocations (Cottrell atmospheres) as well as dislocation pile-ups which may lead to the microcracks formation due to the creation of very high stress concentration at grain boundaries. The results show that the plastic flow discontinuities are related to the Portevin–Le Châtelier phenomenon (PL effect) and they are correlated with the generation of characteristic AE pulse trains. The fractography of broken samples was analyzed on the basis of light (optical), TEM and SEM images.

*Keywords:* lightweight alloys, Acoustic Emission, fracture, Portevin–Le Châtelier phenomenon, twinning, dislocations, shear bands.

### 1. Introduction

Unsatisfying ability to plastic deformation at elevated temperatures, mostly leading to the reduction of deformability and/or hot plasticity is characteristic for many metals and alloys [1-4]. The occurrence of hot-shortness phenomenon, followed by the fracture of intercrystalline character is an important reason for technological difficulties. Previous investigations of the authors of the paper [5-9] of mechanical properties of alloys with the application of AE method were devoted to the Mg-Li-Al alloys and related composites generally in the context of the method of intensive deformation processes leading to their excellent mechanical properties, such as great strength and plasticity or even superplasticity. On the other hand, the investigations of metal and alloy plastic instability using the AE technique were carried out [10-12] mainly in the context of basic aspects of PL effect, twinning or shear band in both poly- and single metal and alloy crystals. The fracture and strengthening properties of Mg-Li based alloys (and composites) were investigated, for example in [13-16], but without the use of AE method, which proved to be a very useful technique of material examination. In this work the results of the investigations of the correlation between the AE phenomenon, the plastic instability, induced by PL

effect, twinning or shear bands, and the both, intergranular and transcrystalline fracture of Mg<sub>4</sub>Li<sub>5</sub>Al and Mg<sub>4</sub>Li<sub>4</sub>Zn alloys subjected to tensile and compression tests at wide range of elevated temperatures are presented.

Alloys based on magnesium with lithium, as the lightest ones from among the known metallic construction materials, are very attractive from the point of view of their application as the materials for light, yet durable constructions to be used in the automotive industry (e.g. car engine housings), light housings of computers and aerospace technology. The basic Mg-Li alloys exist in three phase areas. The hexagonal  $\alpha$  phase appears in the concentration range of Li up to 4 wt.%. If the content of Li is more than 12 wt.% - the  $\beta$  phase of cubic lattice occurs. The alloys of Li content from 4% up to 12 wt.% form the  $\alpha+\beta$  two-phase mixture. The mechanical properties of  $\alpha$  phase are worse from that of the  $\beta$  phase, which is more plastic and thus reveals good machinability and weldability. Alloying additions, e.g. Al (or Zn) from 3% to 5%, slightly increase the density of the alloy, but lead to the precipitation of coherent particles of transition phase,  $\theta$ -MgLi<sub>2</sub>Al/ $\theta$ -MgLi<sub>2</sub>Zn, which additionally strengthens the matrix and leads to the improvement of mechanical properties [14]. The present paper addresses the optical microscopic, as well as TEM and SEM observations of the failure of samples after tensile and compression tests.

\* INSTITUTE OF METALLURGY AND MATERIALS, POLISH ACADEMY OF SCIENCES, 25 REYMONTA STR., 30-059 KRAKÓW, POLAND

\*\* INSTITUTE OF FUNDAMENTAL TECHNOLOGICAL RESEARCH, POLISH ACADEMY OF SCIENCES, 5B PAWINSKIEGO STR., 02-106 WARSZAWA, POLAND

\*\*\* INSTITUTE OF ENGINEERING MATERIALS AND BIOMATERIALS, SILESIAN UNIVERSITY OF TECHNOLOGY, 2A AKADEMICKA STR., 44-100 GLIWICE, POLAND

\*\*\*\* INSTITUTE OF MATERIALS AND MACHINE MECHANICS, 75 RAČIANSKA STR., 830-08 BRATISLAVA, SLOVAK REPUBLIC

# Corresponding author: a.pawelek@imim.pl

## 2. Experimental

### 2.1. Compression and tensile tests

Compression tests were carried out using INSTRON-3382 tensile testing machine, additionally equipped with a specially constructed channel-die which guaranteed plastic flow only in the compression direction (normal direction – ND) and in the direction parallel to the channel axis (elongation direction – ED). In this way the plane state of strains was ensured, since the deformation was impossible in the direction perpendicular to the channel walls (transverse direction – TD). The traverse velocity of the testing machine was 0.05 mm/min what denotes the compression speed of  $10^{-3}\text{s}^{-1}$ . The samples for compression tests had the cubic shape of side 10 mm. The overall look on the testing arrangement and the instrumental details are presented in Fig.1 and Fig.2.

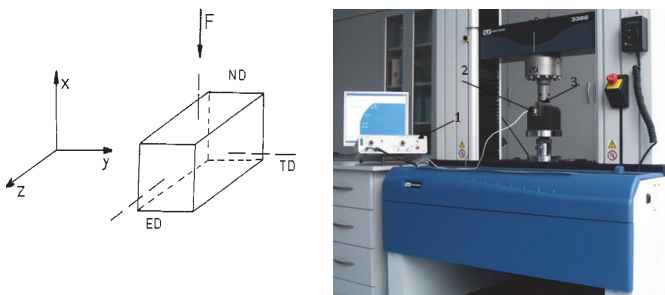


Fig. 1. Left: Schematic view of loading of the sample in the channel-die arrangement, explanation of kinematics' geometry in the text. Right: The experimental set-up used to record the AE signals generated in compressed samples: 1 – AE analyser, 2 - AE sensor, 3 – Channel-die used as sample holder

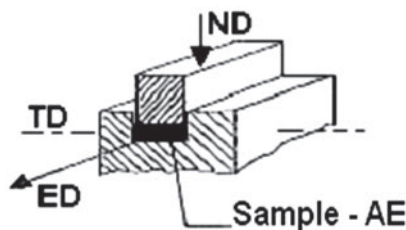


Fig. 2. Details of a channel-die arrangement for compression tests of lightweight alloys, presented in Fig.1

The Mg-Li-Al and Mg-Li-Zn alloys were produced in cooperation with the Institute of Materials and Machine Mechanics of the Slovak Academy of Sciences in Bratislava. The basic Mg-Li alloys were obtained by the method of induction melting of magnesium of 99.99% purity and lithium of 99.5% purity. Series of alloys used in this study were prepared by casting of raw materials in a steel crucible at 800°C with subsequent pouring into a cooled steel mould in a chamber of vacuum induction furnace (Balzers) under low argon pressure (1000 Pa, of 99.999% purity) after previous evacuation ( $10^{-2}$  Pa). The applied preparation procedure was similar to that reported in [15] and used also in our previous works [5-9]. Then, the alloys were machined into standard specimens with rectangular cross-section. The tensile tests at elevated

temperatures were carried out using a special temperature chamber connected with the Zwick 1200 testing machine using a flat dog-bone samples of operating dimensions 2 x 6 mm. The elongation was measured with a laser extensometer. The force was recorded with load cell at 100 kN capacity. A temperature chamber was used to control the test temperature. The specimens were elongated at RT, 50°C, 100°C, 150°C and 200°C. The strain tests were performed at the same speed as the ones mentioned above.

### 2.2. Acoustic emission measurements

The AE method has been applied to the investigations of poly- and single crystals of metals and alloys by the authors of the present paper for many years [5,7,10,17]. The investigations concentrated on explaining the correlations between AE descriptors and the mechanisms of deformation of the materials subjected to the tensile and compression tests. The obtained results allowed the authors to put forward the following thesis: the dominant contribution to the recorded AE signals is derived from the collective movement of many dislocations, associated with their acceleration as well as with the synchronized annihilation of many dislocations, including the annihilation at the free surface of the deformed material.

The measuring system of AE signal was functionally coupled with the stress/strain testing machines and it was described in more details in [5,18]. A broad-band piezoelectric sensor (standard WD type, certified by Physical Acoustics Corporation) enabled to record the acoustic pulses in the frequency range from 100 kHz to 1 MHz. AE signal processing unit was realized with application of the 9812 ADLINK type card hosted in a PC computer. The amplification of the AE analyser was 86 dB and the threshold voltage of the discriminator was 1.17 V. Owing to the suitable software, the analysis of the energy and the time duration of the individual events could be carried out. The dedicated program determined the time of AE event occurrence, its maximum amplitude and the moment of a significant decline of AE signal amplitude.

In the case of compression test the contact between the detector and the sample in a channel-die was maintained by means of a steel rail of a shape of rectangular prism of 100 mm length and 10 x 10 mm cross section which formed a natural waveguide. In order to eliminate the undesired effects of friction against the channel walls, each sample was covered with Teflon foil. Since there was no possibility to place the AE sensor directly in the sample undergoing the tension test in high-temperature chamber therefore the AE sensor was coupled with the lower sample clamp via a steel tape of 2 mm thickness and of 500 mm length. The amplitude and duration of the AE event was measured via analog to the digital acquisition system described above what enabled the calculation of the energy  $E$  of AE events using the approximate formula:

$$E = 0.5 v_{max}^2 \Delta t \quad (1)$$

where  $v_{max}$  was the maximum value of AE signal in the course of the event and  $\Delta t$  was its duration.

### 3. Results and discussion

#### 3.1. Mg<sub>4</sub>Li<sub>5</sub>Al alloys – tensile tests

Figs.3 to 6 show the results of preliminary examinations of the influence of plastic instabilities on the fracture of tensile tested Mg<sub>4</sub>Li<sub>5</sub>Al alloys at room and elevated temperatures: 100°C, 150°C and 200°C together with the corresponding SEM images of fracture.

They show that the plastic instabilities, related to the PL effect, twinning and/or shear band are correlated with the generation of AE events, and affect the final form of fracture. It is necessary to note here that the maximally high AE level at the beginning of the test is related to the yield point (including microplasticity) and it is a result of the creation and operation of dislocation sources. This is a well known fact in literature (see e.g. [8]), and we discuss the AE behaviour after this maximum. Similarly, the high AE peak appearing often at the end of test is related to the breaking of the sample.

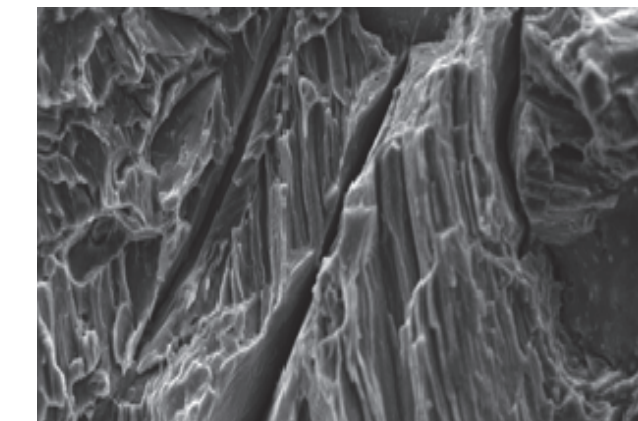
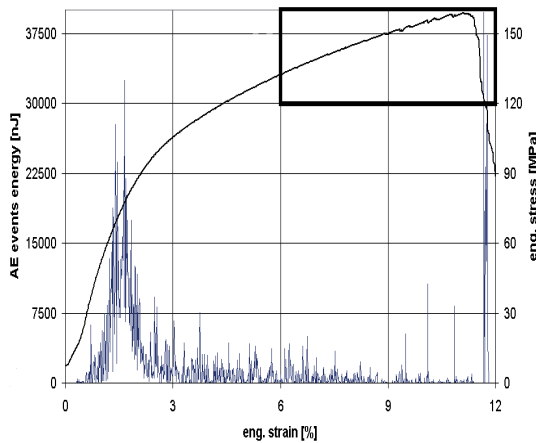


Fig.3. Top: AE events energy and eng. stress versus eng. strain during tensile testing of as-cast Mg<sub>4</sub>Li<sub>5</sub>Al at room temperature. Bottom: The corresponding SEM image of fracture

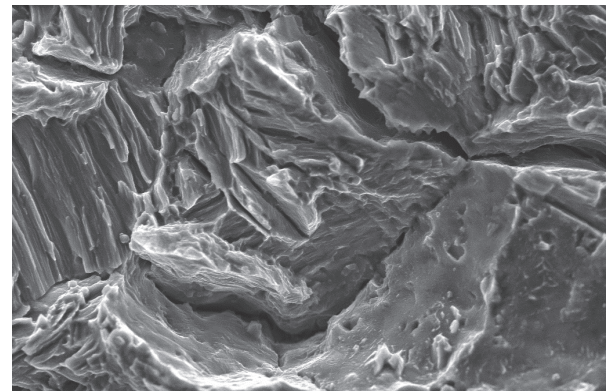
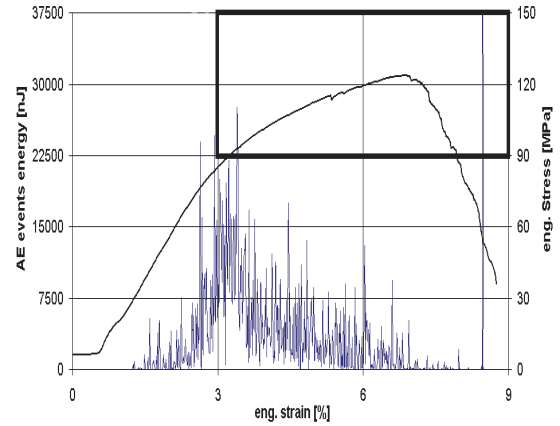


Fig.4. Top: AE event energy and eng. stress versus eng. strain during strain test of Mg<sub>4</sub>Li<sub>5</sub>Al at elevated temperature (100°C). Bottom: corresponding SEM image of fracture.

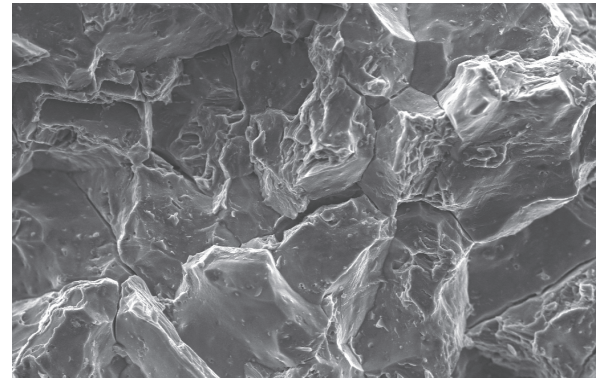
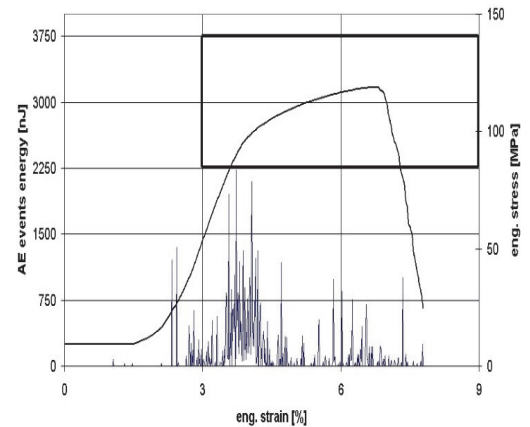


Fig. 5. Top: AE event energy and eng. stress versus eng. strain during strain test of Mg<sub>4</sub>Li<sub>5</sub>Al at elevated temperature (150°C). Bottom: Corresponding SEM image of fracture



The analysis of the AE and PL effects and their relation to the fracture (Figs.3 to 6) is performed with reference to the situation at room temperature (Fig.3), where the fracture is of transcrystalline character. In this case the brittle (fissile) fracture is bound with discontinuities of the fault type and the contribution of surface deformation and traces of intercrystalline fracture. Next, it can be seen in Fig.4, that the AE activity and intensity at 100°C is visibly greater than at room temperature. The fracture type observed in this figure has not essentially changed, and it is still transcrystalline with a distinct contribution of intergranular fracture and traces of surface deformation. However, the behavior of AE has drastically changed at 150°C (Fig.5, AE in scale of tenfold smaller). The both, AE activity and intensity are considerably lower than in the previously discussed cases. The fracture is still transcrystalline, however, cracking along the grain boundaries prevails. The traces of the plastic strain of surface boundary and the single voids and cavities are also observed. From the above analysis we can suppose that the observed changes in the AE behavior may signal the beginning of the transition from one to another kind of fracture.

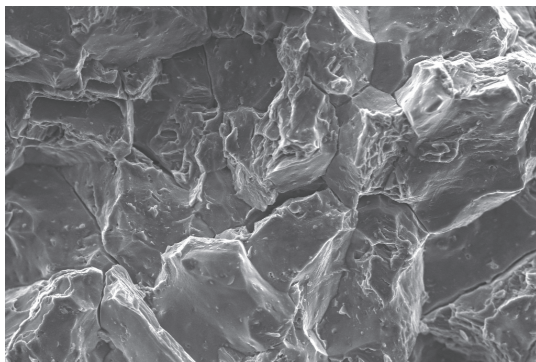
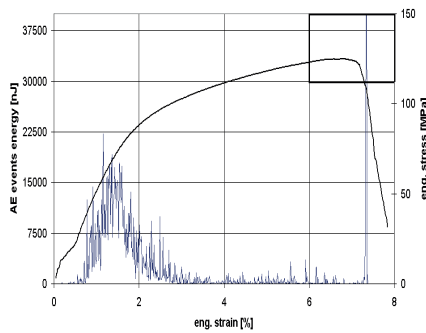


Fig. 6. Top: AE event energy and eng. stress versus eng. strain during strain test of Mg4Li5Al at elevated temperature (200°C). Bottom: Corresponding SEM image of fracture

It seems that this supposition is confirmed by the next observations, illustrated in Fig.6. The AE at 200°C is again of higher level, though slightly lower than earlier, whereas the fracture is of intercrystalline character with a traced contribution of ductile and fissile surfaces. The above presented results may be additionally supported by the calculations of the mean values of the local drops of external stress, total sum of AE event counts and AE event energy calculated in the range of strains (or duration of each compression test) corresponding up to maximal value of external load. The mean energy per one AE event was also calculated. These values are presented in Table 1. It can be seen that all values achieve minimum just at 150°C when the discussed fracture transition is beginning.

It is worth to emphasize here that the relation between the AE activity (AE local peaks) and the PL effect (which accompanies local jumps of external stresses), according to [8,11], may be quite well explained in terms of collective and accelerated movement of many dislocations generated in single slip planes by the sources which are alternately active and blocked by solute atoms (Cottrell atmospheres). It is strongly suggested in papers [6,8,10,11], that also the contribution to AE signals may originate from the synchronized of both, internal and surface annihilation of many dislocations.

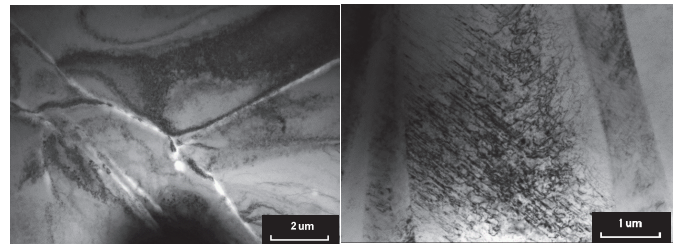


Fig.7. The TEM pictures of Mg4Li5Al alloy after tensile test at 200°C: left – inclusions and microcracks at the region of grain boundary, right – microtwins and inclusions at twin boundaries

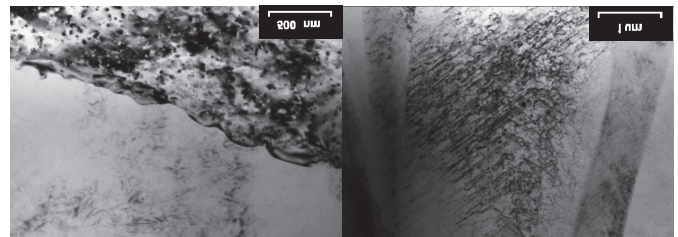


Fig.8. The TEM pictures of Mg4Li5Al alloy after tensile test at 200°C: left – inclusions and microcracks at the region of grain boundary, right – microtwins and inclusions at twin boundaries.

TABLE 1

The stress and AE parameters for Mg4Li5Al alloys tensile tested at elevated temperatures

Mean values → Temperature	Local jumps of external stress [Mp]	Sum of AE event counts	Sum of AE event energy [nJ]	Energy per one AE event [nJ]
RT	0.6	21393	1389000	64,9
100°C	0.8	26696	1780000	66,7
150°C	in errors range	1039	61000	58,7
200°C	0.1	20197	1200000	59,4

Fig.7 and 8 present corresponding TEM pictures observed after tensile tests of Mg4Li5Al alloy at 150°C and 200°C, respectively. It is possible to say generally, that, in the microscale, the changes are not as evident as in the SEM images, which illustrate the fracture changes in the macroscale. The TEM pictures, however, show that the microcracks may be formed due to the stress concentration caused by the condensation of inclusions and/or dislocation assemblies at the grain boundaries. We suppose that these dislocation tangles can be the result of the dislocation pile-up formation which, however, undergo scattering at elevated temperature due to e.g. dislocation climb and/or recovery processes. On the other hand, in the context of plastic deformation, the TEM pictures suggest also that twinning may possibly contribute to the plastic instability, whereas, in turn, the microtwins intersection may also play a role in microcracking occurrence.

### 3.2. Mg4Li5Al – compression tests

The relation between the plastic instability and the fracture was investigated first for the Mg4Li5Al compressed at room temperature. The top of Fig.9 shows the AE behaviour to the break up of the sample. The high AE peak is accompanied with the sample disruption. In this case the fracture of cubic sample occurred along the diagonal surface of the cube (the normal of which lies in the ND-ED plane, see Fig.1). This diagonal plane is generally parallel to the plane of maximal stresses leading to the strain localization and shear band formation, that will be more detail discussed further, in the context of SEM images presented in Fig.10.

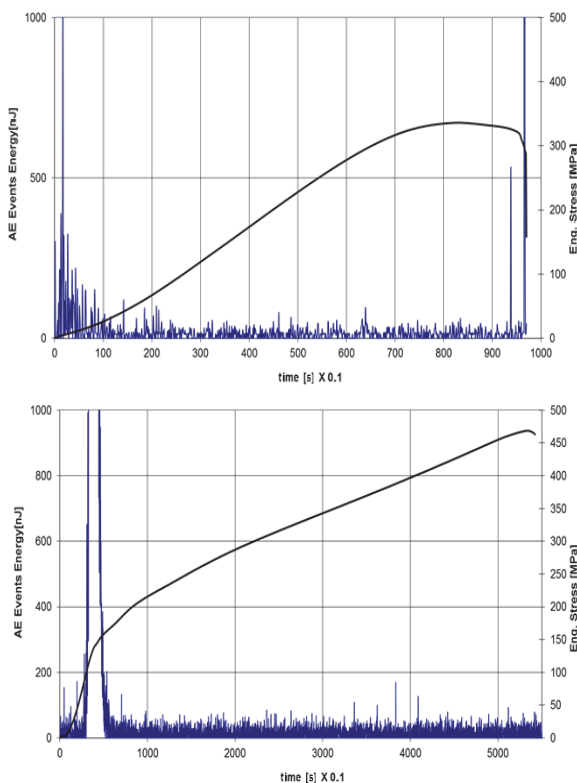


Fig.9: AE behavior and the course of external load: top - up to all-out breaking, bottom – exactly just before breaking of the Mg4Li5Al sample

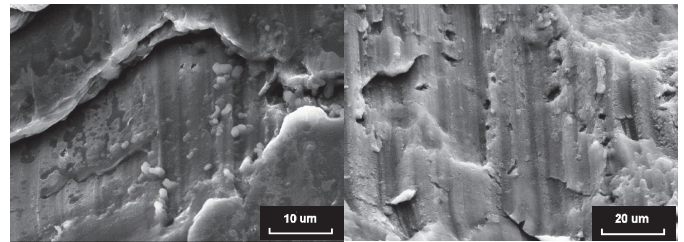


Fig. 10. SEM images of Mg4Li5 Al compressed samples which loading and AE activity vs. time was presented in Fig 9

The essence of idea of the experiment presented in bottom part of Fig. 9 was based on a precise compression of another sample up to the moment just before the previous sample had broken. The fracture surface for the SEM observation was obtained in this case by manual breakdown of the sample. The corresponding SEM image of the fracture (Fig. 10, right side) shows, that the length of crack path is visibly shorter than in the case observed at left side of Fig.10. It means that the final break of the sample is a result of successive growth of the length of crack path.

On the other hand Fig.11a shows a fully developed shear band, which is observed on the side wall (parallel to ND-ED plane) of cubic sample compressed up to adequate external loading. Additionally, Fig.11b shows that the fully formed shear bands may be realized by the development of slip bands and next microshear bands which cut cross many grains, what means that the final fracture in this case is of transcrystalline character.

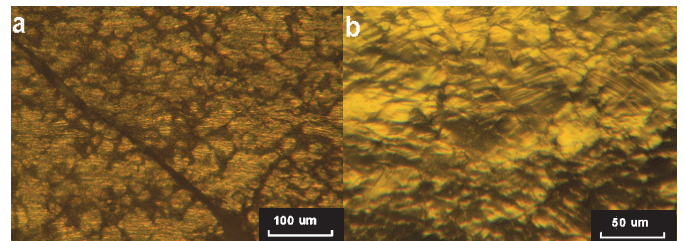


Fig.11: Optical images illustrating the fully developed shear band (a) and the slip bands and microshear bands crossing over many grains (b)

### 3.3. Mg4Li4Zn alloys – tensile tests

In order to investigate the role of alloy addition, e.g. of zinc instead aluminium, a Mg4Li4Zn alloy was chosen, especially because the plastic instability connected with the PL effect in these alloys is known in literature [19]. The results of the preliminary studies for these alloys are presented below in Fig.12. AE behavior and external stress are shown for room temperature and for 200°C. Two SEM images of the fracture at room and 200 °C temperatures are presented respectively in Fig.13 whereas in Fig.14 the SEM pictures demonstrate the additional observations related to the fracture at 400°C.

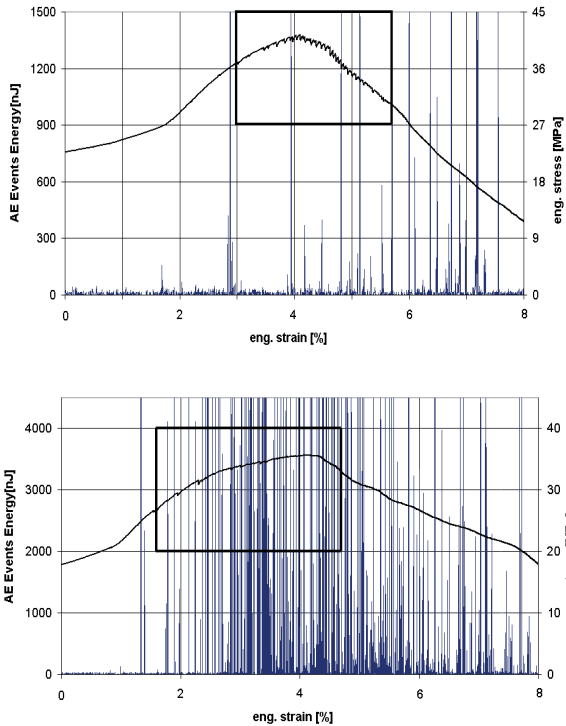


Fig. 12. AE behavior and the external stresses of tensile tested Mg4Li4Zn alloy: top - at room temperature and bottom - at 200°C

Moreover, it is visible on Fig.12 that the first appearing high AE peaks – about  $\varepsilon \approx 3\%$ , on top, and about 700s (or  $\varepsilon \approx 2\%$ ), on bottom – can define the critical strain  $\varepsilon_c$ , which according [11], determines the beginning of the locking of dislocation sources by Cottrell atmospheres, and next their unlocking that leads to the active slip accompanied by the generation of elastic waves.

On the other hand it has been found that both the Acoustic Emission and the drops of the force observed at stress-strain curve presented in upper part of Fig.12 are of regular shape of pulse trains. The drops of the stress presented in Fig.12 are of amplitude of ca. 2 MPa and this amplitude is approximately twice as high as that presented in Fig.6 and occurring in Mg4Li5Al alloy. One can mention that the oscillation of the stress is of high frequency of ca. one drop per 5 second during the test performed at room temperature. The stress oscillation observed at 200°C is characterised by lower frequency denoting one drop per 100 second and lower amplitude of approx. 1 MPa. However the oscillations registered at stress-strain curve during the tensile tests of Mg4Li4Zn alloy are more readable than those registered in Mg4Li5Al alloy.

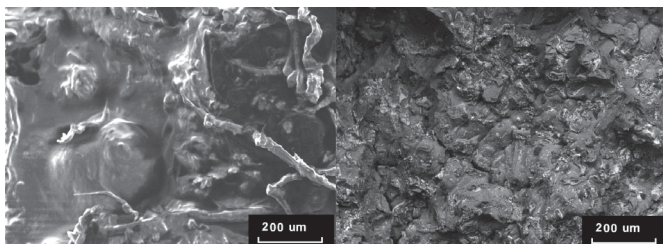


Fig.13. SEM images of fracture of tensile tested Mg4Li4Zn alloy left - at room temperature, right - at 200°C

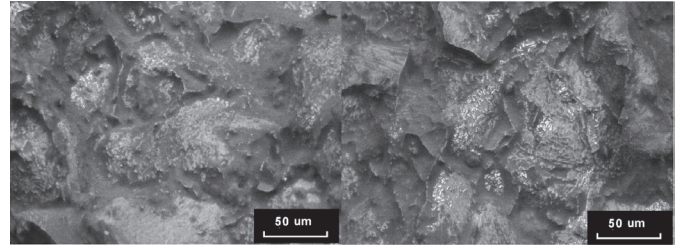


Fig.14. SEM images of fracture of tensile tested Mg4Li4Zn alloy at 400°C

#### 4. Conclusion

The work describes the preliminary research of the influence of plastic instabilities (PL effect, twinning, shear banding) on the fracture of Mg-Li based alloys in tensile and compression tests at elevated temperatures with the unique application of Acoustic Emission technique. It seems that the following conclusions are quite reasonable:

1. The fractures of tensile tested Mg4Li5Al alloys at elevated temperatures are initially of transcrystalline character but the transition to intergranular type starts already from 150°C, while at 200°C the fracture changes its character into intercrystalline.
2. The transition from one to another kind of fracture is correlated with the stress and AE parameters achieve minimal values just at the same temperature 150°C.
3. The AE technique can be helpful in further research of the changes in fracture character at elevated and/or higher temperatures in a way of tracing the changes of emitted AE energy.
4. The fracture of compressed Mg4Li5Al alloy at room temperature is related to the strain localization in shear bands, and it is characterized by growth and development of the crack path.
5. In Mg4Li4Zn alloys tensile tested at room and elevated temperature, character, and the fracture, being mostly of intergranular character, as well as the AE behavior are not essentially changed.
6. The oscillations registered at stress-strain curve during the tensile tests were more readable and were of higher amplitude in the case if loading of Mg4Li4Zn alloy when comparing to those observed at loading of Mg4Li5Al alloy in the same conditions.

#### Acknowledgments

The studies were financially supported by Polish National Science Centre (project in competition OPUS 4, grant No 2012/07/B/ST8/03055), and also by the Slovak Academy of Sciences - project VEGA No 2/0186/14.

#### REFERENCES

- [1] S. Fujiwara, K. Abiko, Journal de Phys. IV, Coll. C7, C7-295 (1995).



- [2] K. Misra, S. Prasad, *Mat. Sci.* **35**, 3321(2000), DOI: 10.1007/s10853-011-5728-9.
- [3] M. Kanno, N. Shimodaira, *Scripta Metall.* **21**, 1487 (1987).
- [4] H. Yamagata, O. Izumi, *J. Jap. Inst. Metals* **42**, 1012 (1978).
- [5] S. Kudela, A. Pawełek, Z. Ranachowski, A. Piątkowski, S. Kudela Jr., P. Ranachowski, *Kovove Mater.* **49**, 271 (2011), DOI: 10.4149/km 2011 4 271.
- [6] A. Pawełek, Z. Jasiński, S. Kudela, A. Piątkowski, P. Ranachowski, F. Rejmund, F., Acoustic emission in channel-die compressed Mg-Li-Al alloys reinforced with short ceramic fibres and ibidem Influence of  $\beta$  phase on mechanical and acoustic behaviour of Mg-Li-Al alloys in: J. Jerz, P. Šebo, M. Zemankova (Ed.), *Proceedings of the Int. Conf. on Advanced Metallic Materials*, Smolenice, Slovakia, November 5-7, 2003, Slovak Acad. of Sciences (2003)
- [7] J. Kuśnierz, A. Pawełek, Z. Ranachowski, A. Piątkowski, Z. Jasiński, S. Kudela, S. Kúdela Jr., *Rev. Adv. Mater. Sci.* **18**, 583 (2008).
- [8] A. Pawełek, Mechanical behavior and plastic instabilities of compressed Al metals and alloys investigated with application of intensive strain and acoustic emission methods, in: Z. Ahmad (Ed.), *Recent Trends in Processing and Degradation of Aluminium Alloys 2011*, InTech (2011).
- [9] A. Pawełek, W. Ozgowicz, Z. Ranachowski, S. Kudela, A. Piątkowski, S. Kúdela Jr., P. Ranachowski, *Mater. Tehnol.* (2015), DOI: 10.1007/s10973-011-1375-2 (in press).
- [10] A. Pawełek, A. Piątkowski, Z. Jasiński, S. Pilecki, *Z. Metallkde.* **92**, 376 (2001).
- [11] A. Pawełek, *Z. Metallkde.* **80**, 614 (1989).
- [12] Z. Jasiński, A. Pawełek, A. Piątkowski, Z. Ranachowski, *Arch. Metall. Mater.* **54**, 29 (2009), DOI: 10.3139/146.110033.
- [13] S. Kúdela Jr., H. Wendrock, S. Kúdela, A. Pawełek, A. Piątkowski i K. Wetzig, *Int. J. of Mat. Res.*, **100**, 910 (2009), DOI: 10.3139/146.110127
- [14] S. Kúdela, *Int. J. Mat. Prod. Techn.* **18**, 91(2003).
- [15] S. Kamado, Y. Kojima, *Met. Sci. Techn.* **16**, 45 (1998).
- [16] M. E.Mehtedi, S. Spigarelli, E. Evangelista, G. Rosen, *Int. J. of Mat. Res.* **100**, 447 (2009), DOI: 10.3139/146.110033.
- [17] A. Pawełek, A. Piątkowski, S. Kudela, Z. Jasiński, *Arch. Metall. Mater.* **51**, 245 (2006), DOI: 10.3139/146.110033.
- [18] M. Ohtsu, *Sensor and Instrument*, in: Ch. U. Grosse, M. Ohtsu (Ed.), *Acoustic Emission Testing*, 2008, Springer (2008), DOI: 10.1007/978-3-540-69972-9
- [19] C. Wang, Z. Li, Y. Xu, E. Han, *J. Mater. Sci.* **42**, 3573 (2007), DOI: 10.1007/s10853-011-5728-9.

